Supplementary Information

Title

Superior cycling stability of Zr-Hf-Co-Fe-Ni hydrogen isotope storage alloys achieved by hydrogen binding energy modulation

S1. Supplementary Methods

S1.1 Van't Hoff equation.

Based on the pressure-composition-temperature (PCT) curves, the relevant thermodynamic parameters are calculated by Van't Hoff equation as shown follows:

$$\ln P_{eq} = -\Delta H/RT + \Delta S/R \quad (1)$$

where R is the molar gas constant, P_{eq}, ΔH, ΔS, and T represent the equilibrium de-/hydrogenation pressure, enthalpy change, entropy change and testing temperature of the sample, respectively.

S1.2 The calculation equation for the hydrogen binding energy.

The hydrogen binding energy ($E_{H\text{-}binding}$) representing the energy needed to detach an H atom from a crystal cell, which can be calculated by the following equation:

$$E_{H\text{-}binding} = E_1 + E_H - E_0 \quad (2)$$

where E_H is the energy of a H atom, the energies of the optimized structure with and without the removal of a H atom are denoted by E_1 and E_0, respectively.

S2. Supplementary Figures

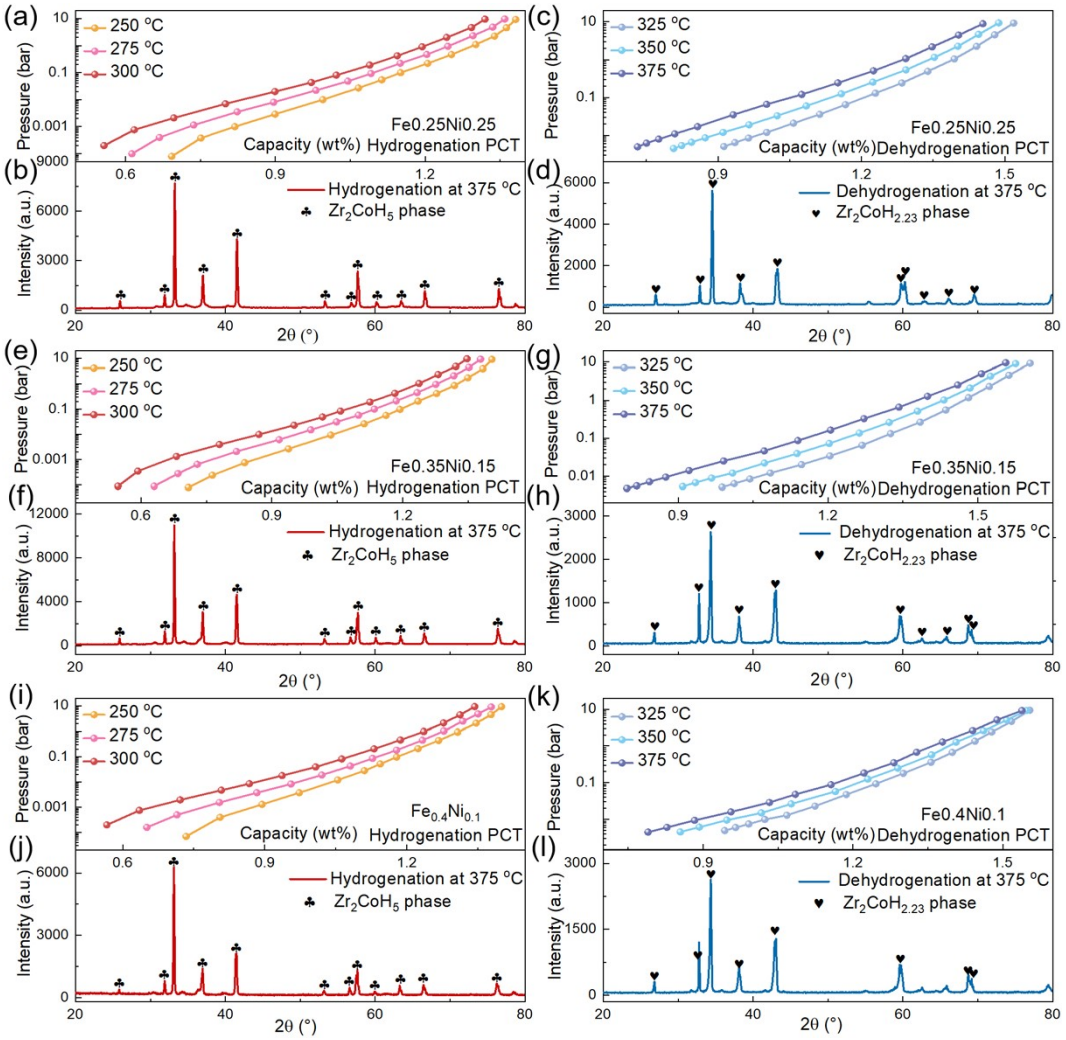

Fig. S1. The hydrogenation (a, e, i) and dehydrogenation (c, g, k) PCT curves, XRD patterns of hydrogenation samples after 250 °C PCT test (b, f, j) and dehydrogenation samples after 375 °C PCT test (d, h, l) of $Zr_{1.5}Hf_{0.5}Co_{0.5}Fe_xNi_{0.5-x}$ (x = 0.25, 0.3, 0.35, 0.4) alloys.

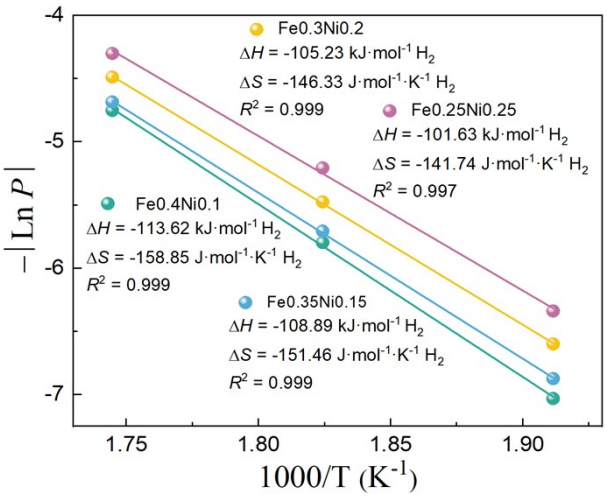

Fig. S2. Van't Hoff plots for hydrogenation PCT curves of $Zr_{1.5}Hf_{0.5}Co_{0.5}Fe_xNi_{0.5-x}$ (x = 0.25, 0.3, 0.35, 0.4) alloys.

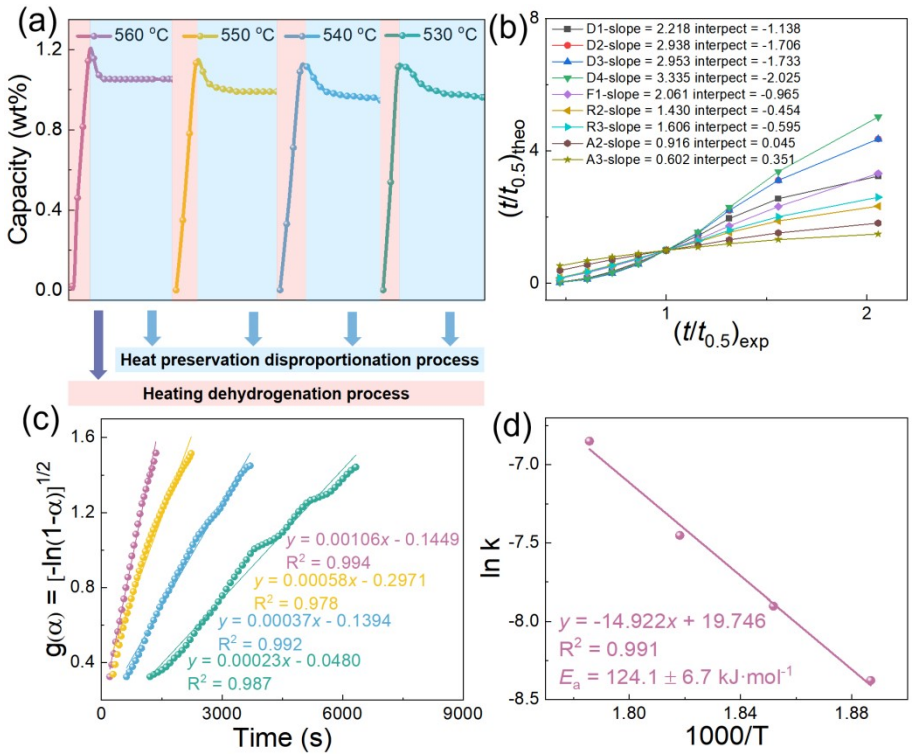

Fig. S3. The disproportionation kinetic curves of $Zr_{1.5}Hf_{0.5}Co_{0.5}Fe_{0.25}Ni_{0.25}$ sample (a), comparison of 9 different kinetic models with disproportionation kinetic curves (b), fitting results of disproportionation kinetic curves with A2 model (c), and activation energy calculation using Arrhenius plot (d).

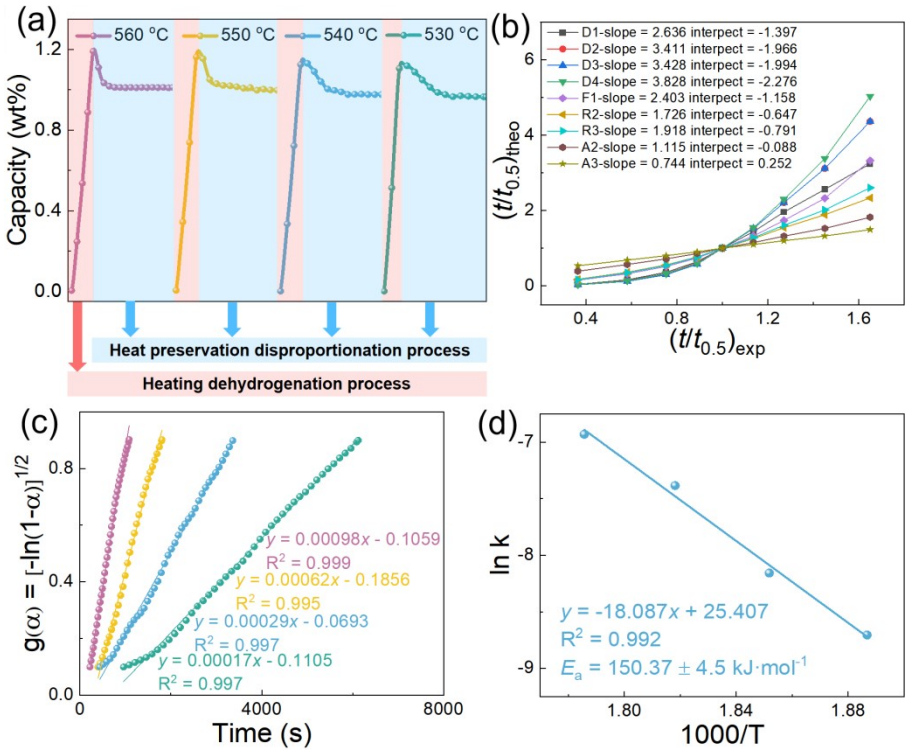

Fig. S4. The disproportionation kinetic curves of $Zr_{1.5}Hf_{0.5}Co_{0.5}Fe_{0.35}Ni_{0.15}$ sample (a), comparison of 9 different kinetic models with disproportionation kinetic curves (b), fitting results of disproportionation kinetic curves with A2 model (c), and activation energy calculation using Arrhenius plot (d).

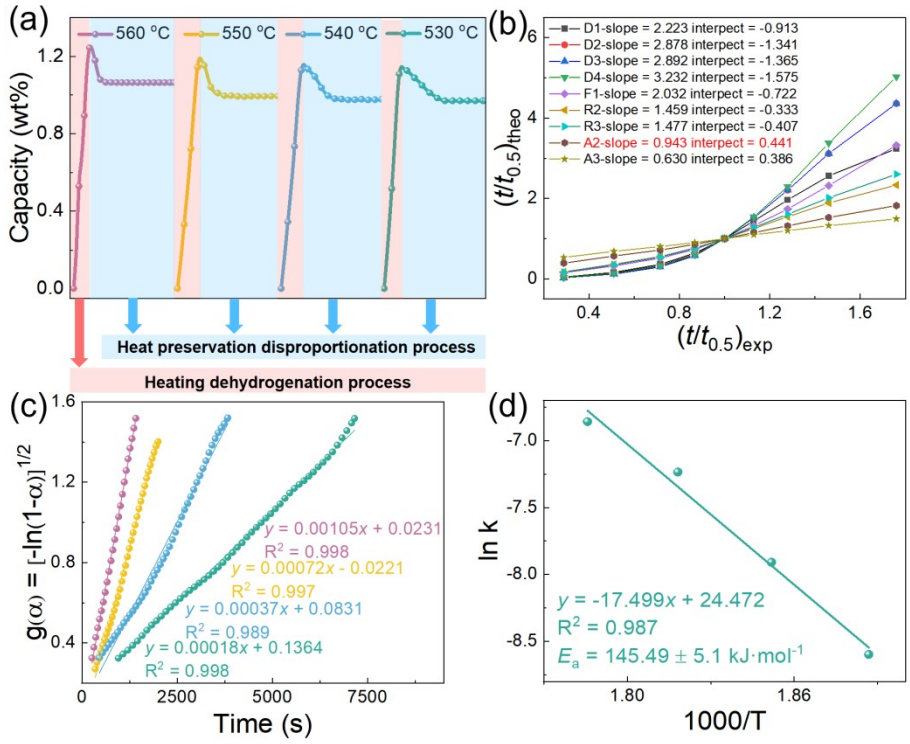

Fig. S5. The disproportionation kinetic curves of $Zr_{1.5}Hf_{0.5}Co_{0.5}Fe_{0.4}Ni_{0.1}$ sample (a), comparison of 9 different kinetic models with disproportionation kinetic curves (b), fitting results of disproportionation kinetic curves with A2 model (c), and activation energy calculation using Arrhenius plot (d).

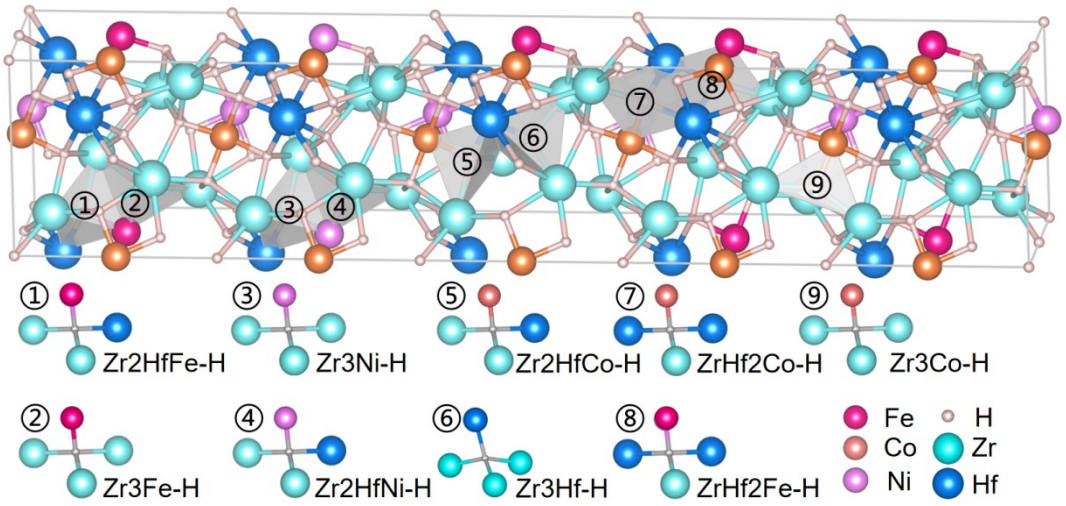

Fig. S6. The unit cell structure of $Zr_{1.5}Hf_{0.5}Co_{0.5}Fe_{0.3}Ni_{0.2}$ hydride and the schematic diagram of corresponding hydrogen storage interstitial sites.

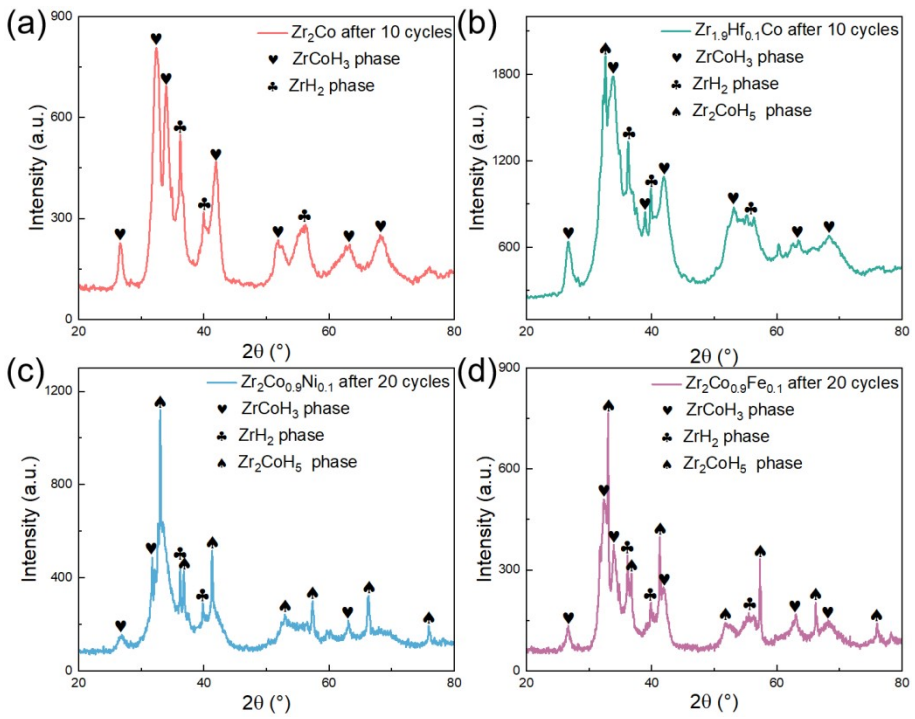

Fig. S7. XRD patterns of Zr_2Co (a) and $Zr_{1.9}Hf_{0.1}Co$ (b) samples after 10 cycles; XRD patterns of $Zr_2Co_{0.9}Fe_{0.1}$ (c) and $Zr_2Co_{0.9}Ni_{0.1}$ (d) samples after 20 cycles.